Selected Spectroscopic Results on Element 115 Decay Chains

Rudolph, Dirk; Forsberg, Ulrika; Golubev, Pavel; Sarmiento, Luis; Yakushev, A.; Andersson, L.-L.; Di Nitto, A.; Düllmann, Ch.E.; Gates, J.M.; Gregorich, K.E.; Gross, C.J.; Herzberg, R.-D.; Heßberger, F.P.; Khuyagbaatar, J.; Kratz, J.V.; Rykaczewski, K.; Schädel, M.; Åberg, Sven; Ackermann, D.; Block, M.; Brand, H.; Carlsson, Gillis; Cox, D.; Derkx, X.; Eberhardt, K.; Even, J.; Fahlander, Claes; Gerl, J.; Jäger, E.; Kindler, B.; Krier, J.; Kojouharov, I.; Kurz, N.; Lommel, B.; Mistry, A.; Mokry, C.; Nitsche, H.; Omtvedt, J.P.; Papadakis, P.; Ragnarsson, Ingemar; Runke, J.; Schaffner, H.; Schausten, B.; Thörle-Pospiech, P.; Torres, T.; Traut, T.; Trautmann, N.; Türler, A.; Ward, A.; Ward, Daniel

Published in:
Journal of Radioanalytical and Nuclear Chemistry

DOI:
10.1007/s10967-014-3445-y

2015

LUND UNIVERSITY

PO Box 117
221 00 Lund
+46 46-222 00 00

Selected Spectroscopic Results on Element 115 Decay Chains

D. Rudolph,[1,*] U. Forsberg,[1] P. Golubev,[1] L.G. Sarmiento,[1] A. Yakushev,[2] L.-L. Andersson,[3] A. Di Nitto,[4] Ch.E. Düllmann,[2,3,4] J.M. Gates,[5] K.E. Gregorich,[5] C.J. Gross,[6] R.-D. Herzberg,[7] F.P. Heßberger,[2,3] J. Khuyagbaatar,[3] J.V. Kratz,[4] K. Rykaczewski,[6] M. Schädel,[2,8] S. Åberg,[1] D. Ackermann,[2] M. Block,[2] H. Brand,[2] B.G. Carlsson,[1] D. Cox,[7] X. Derkx,[3,4] K. Eberhardt,[3,4] J. Even,[3] C. Fahlander,[1] J. Gerl,[2] E. Jäger,[2] B. Kindler,[2] J. Krier,[2] I. Kojouharov,[2] N. Kurz,[2] B. Lommel,[2] A. Mistry,[7] C. Mokry,[3,4] H. Nitsche,[5] J.P. Omtvedt,[9] P. Papadakis,[7] I. Ragnarsson,[1] J. Runke,[2] H. Schaffner,[2] B. Schausten,[2] P. Thörle-Pospiech,[3,4] T. Torres,[2] T. Traut,[4] N. Trautmann,[4] A. Türler,[10] A. Ward,[7] D.E. Ward,[1] N. Wiehl,[3,4]

[1] *Lund University, 22100 Lund, Sweden*

[2] *GSI Helmholtzzentrum für Schwerionenforschung GmbH, 64291 Darmstadt, Germany*

[3] *Helmholtz Institute Mainz, 55099 Mainz, Germany*

[4] *Johannes Gutenberg-Universität Mainz, 55099 Mainz, Germany*

[5] *Lawrence Berkeley National Laboratory, Berkeley, CA 94720, USA*

[6] *Oak Ridge National Laboratory, Oak Ridge, TN 37831, USA*

[7] *University of Liverpool, Liverpool L69 7ZE, United Kingdom*

[8] *Advanced Science Research Center,*
Japan Atomic Energy Agency, Tokai, Japan

[9] *University of Oslo, 0315 Oslo, Norway and*

[10] *Paul Scherrer Institute and University of Bern, CH-5232 Villigen, Switzerland*

(Dated: August 8, 2014)

* Dirk.Rudolph@nuclear.lu.se

Abstract

Thirty correlated α-decay chains were observed in an experiment studying the fusion-evaporation reaction ^{48}Ca + ^{243}Am at the GSI Helmholtzzentrum für Schwerionenforschung. The decay characteristics of the majority of these 30 chains are consistent with previous observations and interpretations of such chains to originate from isotopes of element $Z = 115$. High-resolution α-photon coincidence spectroscopy in conjunction with comprehensive Monte-Carlo simulations allow to propose excitation schemes of atomic nuclei of the heaviest elements, thereby probing nuclear structure models near the 'Island of Stability' with unprecedented experimental precision.

PACS numbers: 21.10.-k,23.20.Lv,23.60+e,27.90.+b

More than 40 years ago, an 'Island of Stability' of superheavy nuclei was predicted by nuclear structure theorists [1]. This island rests on increased nuclear stability due to anticipated magic proton and neutron numbers at spherical nuclear shape (see, e.g., Ref. [2]), while surrounding archipelagos may also arise from increased nuclear binding of deformed atomic nuclei [3, 4]. Over the years, experimentalists have come closer and closer to the 'Island of Stability', and along their way they have not only been producing heavier and heavier atomic nuclei, but also added more and more chemical elements to Mendeleev's Periodic Table.

During the past decade, correlated α-decay chains have been observed in a number of experiments performed at the Flerov Laboratory of Nuclear Reactions (FLNR) in Dubna, Russia. Beams of ^{48}Ca (Z = 20) impinged on actinide targets (Z = 92-98). The decay chains were interpreted to start from isotopes of elements Z = 112-118, produced via the mechanism of fusion-evaporation reactions [5–7]. The discovery of elements Z = 114, Fl, and Z = 116, Lv, was acknowledged in 2011 by IUPAC's and IUPAP's Joint Working Party [8]. One reason amongst several concerns α-decay energies of even-even nuclei along a decay chain, which are characteristic for a given decay step and which were independently confirmed in the mean time [9–13].

The decay pattern is usually more complex for α decays of odd-A or especially odd-odd nuclei, because they usually proceed to excited states in the daughter nucleus [14, 15]. On the one hand, this hampers indirect methods of determining Z, not least because decay chains along the same isotopes may follow different decay paths depending on the starting point of a certain isotopic decay sequence. On the other hand, the possibility arises to observe X ray photons in the course of the electromagnetic internal conversion decays of the excited states in α-decay daughter nuclei [16]. X-ray energies are predicted with high precision even for the heaviest elements since long (e.g. Ref. [17]), and they are characteristic for a given proton, hence atomic number [18]. In addition, high-resolution α-photon coincidence spectroscopy such as performed on element $Z = 115$ decay chains closes in towards nuclear structure studies near the 'Island of Stability' [19].

The experiment was performed at the GSI Helmholtzzentrum für Schwerionenforschung in Darmstadt, Germany. The UNILAC facility provided a beam of time-averaged 6×10^{12} ^{48}Ca^{8+} ions per second at energies of 5.400 and 5.462 MeV/u, i.e. roughly 10% of the speed of light. A beam integral of 6×10^{18} Ca ions was collected in three weeks. In front of the gas-filled separator TASCA [22], the heavy-ion beam hit one of four target segments mounted on a rotating target wheel. The segments carried on average 0.83 $\mathrm{mg\,cm^{-2}}$ thick layers of $^{243}Am_2O_3$ electroplated onto a titanium support foil [23]. The fusion-evaporation residues were focused towards the TASISpec radiation detector system [24] positioned at the focal plane of TASCA. On the order of 100 charged particles per second reached the 32×32-strip double-sided silicon strip DSSSD implantation detector, which is 6×6 cm^2 in area and 0.52 mm thick and visible in the photograph of the 'open' TASISpec in Fig. 1(a). Together with the implantation DSSSD, four additional DSSSDs of the same size and placed upstream form effectively a cube of $32\times32+4\times16\times16=2048$ silicon pixels for charged-particle detection. During the experiment, this cube is housed inside a 0.5-1.0 mm thin aluminum box, and each of the five DSSSDs is backed up by a composite germanium detector of either Clover- or Cluster-type for photon detection. These detectors comprise either four or seven Ge crystals, while the combined Si-Ge arrangement gives rise to unprecedentedly high α-photon coincidence efficiency.

The charged particles reaching the implantation DSSSD and those due to subsequent radioactive decays trigger the data acquisition. Position and time correlations of implanted ions and their decays are subsequently being searched for in the data, which in the present case has a volume in excess of 2 TB accounting for 1.5×10^8 stored events. In this haystack, in total 30 correlated α-decay chains could be discriminated and attributed to the observation of three isotopes of element $Z = 115$ [19, 25–27].

For instance, Fig. 1(b) shows the result of 53 correlated decay chains associated with the production and decay of the isotope ^{288}115. The averages are based on 22 of the 30 individual chains from our experiment [19] merged with 31 chains from studies by Oganessian *et al.* [20, 21]. In fact, this decay chain in Fig. 1(b) is the hitherto best studied of all those produced in any of the ^{48}Ca-plus-actinide-target reactions [5–7]; not only in terms of plain statistics, but thanks to our experiment also in view of spectroscopic precision. This is highlighted by having measured the first α-γ coincidences and α-X-ray candidates for Z identification of these very heavy nuclei [19].

In several publications, more details can be found on the preparations of our experiment [28, 29], its set-up [24], the experiment itself [19, 25], data analysis procedures [26] as well as discussions related to the remaining $30 - 22 = 8$ chains also associated with isotopes of element $Z = 115$ [25].

In the following, the focus lies on the α-decay of $^{288}115$ and more general Q_α values along the decay chain starting with that isotope. Figure 2 compares experimental data associated with the α decay $^{288}115 \rightarrow ^{284}113$ [panels (d) and (e)] with results from GEANT4 Monte-Carlo simulations [panels (a)-(c)] using the corresponding proposed decay schemes displayed in Fig. 3(a)-(c).

The experimental spectrum in Fig. 2(d) provides the energy measurements of nine so-called 'full-energy' $^{288}115$ decay events in the TASISpec implantation DSSSD together with five so-called 'reconstructed' $^{288}115$ decay events. In case of the latter, the α particle leaves part of its energy in the implantation DSSSD before it comes to rest in one of the four upstream DSSSD detectors. In panel (e), 21 more full-energy events from Refs. [20, 21] are added. Since different energy measurements are associated with different uncertainties and because reconstructed events naturally are less precise (cf. Ref. [28]), the various single counts in panels (d) and (e) do not have equal weight in the energy domain. To account for this issue, each count in the spectrum can be best replaced by a Gaussian distribution with the centroid being the measured energy and the width corresponding to the reported uncertainty, as they are listed in the respective tables of Refs. [19, 21]. The continuous energy distribution in panel (e) thus represents the sum of these Gaussian-shaped distributions. In any case, the most prominent feature of the experimental data displayed in Fig. 2(d) and (e) is the *absence* of a single, dominant α line — if there were, for instance, a single ground state-to-ground state α decay, all events together would rather form a peak-like structure with a full width at half maximum (FWHM) of ~ 50 keV. This is obviously not the case.

Consequently, one or several α decays into excited states of $^{284}113$ have to be considered. Excited states typically continue to decay towards the nuclear ground state by electromagnetic radiation, i.e. either by emitting γ rays or by internal conversion. The latter is generally much more likely for low-energy transitions in superheavy nuclei [30]. Since the time difference between α decay and subsequent electromagnetic decay is usually confined to a few hundred nanoseconds (denoted as 'prompt coincidence'), neither the DSSSD itself nor its conventional read-out electronics is able to distinguish between signals from α-particle or conversion electron interactions in a given pixel of the DSSSD. This leads to summing of α-particle and conversion electron energies, either fully or partially, and in the end follows a broadened distribution of measured energies [31] — like the experimental one observed in Fig. 2(d) and (e).

For complex decay schemes such as those in Fig. 3 the resulting energy spectrum is practically impossible to assess ‘by hand’, simply because there are too many options of, e.g., conversion or γ-ray decay probabilities, or full or partial detection probabilities for a series of conversion electrons. Instead, we developed a TASISpec detector system in virtual GEANT4 Monte Carlo space, which allows us to simulate the TASISpec response to as many as considered necessary, virtual element 115 decays [32, 33].

Three different decay scenarios with varying ground state-to-ground state Q_α values are shown and investigated in Figs. 2 and 3. Panels (a)-(c) in Fig. 2 provide the arbitrarily normalized results of 100000 simulated decays of the corresponding $^{288}115$ decay schemes in Fig. 3. As a starting point, a single α decay into an excited state of 290 keV is assumed, which cascades towards the ground state by four highly converted transitions is discussed for three Q_α values in panels (a). Four equally intense α-particle decays into the four excited states are presented in panels (b) exploring two Q_α values. A rather simple case with an α-decay into one excited state at 105 keV is illustrated by panels (c). The decay of 105 keV is highlighted because one 105 keV γ may have been observed in prompt coincidence with a $^{288}115$ α decay [19, 25].

Clearly, option (c) yields a too narrow energy spectrum, while options (a) and (b) lead already to reasonably broad simulated energy distributions. Furthermore, options (a) and (b) are not distinguishable based on the existing data, while it is easily feasible to adjust the centroid of the simulated distribution to the observed distribution by chosing a proper Q_α value; $Q_\alpha \sim 10.75$ MeV in case (a) and $Q_\alpha \sim 10.70$ MeV in case (b). These estimates are based on the position of the centroids of the distributions in Fig. 2.

To achieve even further improved agreement of the simulations in, e.g., Fig. 2(a), with the somewhat broader experimental distribution in Fig. 2(e), more phase space for electromagnetic decay may have to be added on the cost of α-particle decay energy. Such kind of self consistency between the simulated spectral response and the observed spectra for a certain physics input, i.e. decay scenario, is going to add significant confidence to the respective physics result. Here, $Q_\alpha = 10.75(10)$ MeV can already be safely inferred for the α decay of $^{288}115$.

Applying the procedure described above also to the other four Q_α values along the $^{288}115$ decay chain provides the experimental values in Fig. 4 (black dots); $Q_\alpha = 10.30(10)$ MeV follows for the decay of $^{284}113$, which shows a pattern similar to $^{288}115$. For ^{280}Rg, ^{276}Mt, and ^{272}Bh discrete α-γ coincidences and/or apparent peaks in the particle energy spectrum constrain the values even more: $Q_\alpha = 10.15(1)$, 10.10(1), and 9.21(1) MeV, respectively [19]. Due to our high-resolution coincidence technique and Monte-Carlo cross-check, the numbers are much more precise than previous *estimates* of Q_α values of these odd-odd nuclei.

Figure 4 compares the experimental Q_α results with a number of theoretical predictions using different types of nuclear structure models [34–38]. All models essentially agree that ^{276}Mt, ^{272}Bh, and ^{268}Db exhibit rather constant quadrupole deformed shapes with a basic deformation parameter of $\beta_2 \sim 0.2$. ^{280}Rg is predicted slightly less deformed, while the predictions at the beginning of the chain range from slightly oblate via near-spherical towards almost prolate superdeformed. Indeed, the Q_α values of the lighter members of the chain are rather well described by almost all the models, which provides confidence that these nuclei are in fact moderately prolate deformed. Interestingly, however, none of the models appears to be able to describe the complete sequence from ^{288}115 via ^{284}113 to ^{280}Rg, i.e. the regime where *different* shapes are predicted. Since these differences have their origin in the underlying shell structure, in particular the amount of magicity or size of the shell gap at $Z = 114$, it will be interesting to see which model and/or which parametrisation is going to yield a consistent description of all Q_α values along the ^{288}115 chain. One experimental note of caution must be added though: It cannot be excluded that the decay chain starts from an *excited* isomeric state in ^{288}115. While this can in principle lead to a too high – but not too low – experimental Q_α value somewhere else in the chain, the discrepancy of more than 400 keV at ^{284}113 between experiment and lower-lying theoretical numbers seems difficult to be solely attributed to this explanation. Certainly, more dedicated nuclear structure assessments need to be performed, including possible Nilsson-orbit occupancies of the unpaired proton and neutron along the ^{288}115 decay chain.

"In conclusion, thirty correlated α-decay chains were observed following the reaction ^{48}Ca+^{243}Am. Decay schemes arising from high-resolution spectroscopic coincidence data, in conjunction with comprehensive Monte-Carlo simulations, open the door for direct nuclear structure insights of these heaviest man-made atomic nuclei. Previous assignments linking the majority of the decay chains to the decay of ^{287,288}115 [20, 21] are confirmed" [19]. These features are exemplified by a concise study of the α-decay properties of ^{288}115 and its implication on predicted Q_α values.

The authors would like to thank the ion-source and accelerator staff at GSI. This work is supported by the European Community FP7 – Capacities ENSAR No. 262010, the Royal Physiographic Society in Lund, the Euroball Owners Committee, the Swedish Research Council, the German BMBF, the Office of Nuclear Physics, U.S. Department of Energy, and the UK Science and Technology Facilities Council.

---

[1] Nilsson SG, Tsang CF, Sobiczewski A, Szymański Z, Wycech S, Gustafson C, Lamm I-L, Möller P, Nilsson B (1969) Nucl Phys A131:1-66

[2] Bender M, Nazarewicz W, Reinhard P-G (2001) Phys Lett B515:42-48

[3] Ćwiok S, Heenen PH, Nazarewicz W (2005) Nature 433:705-709

[4] Dvorak J, Brüchle W, Chelnokov M, Dressler R, Düllmann CE, Eberhardt K, Gorshkov V, Jäger E, Krücken R, Kuznetsov A, Nagame Y, Nebel F, Novackova Z, Qin Z, Schädel M, Schausten B, Schimpf E, Semchenkov A, Thörle P, Türler A, Wegrzecki M, Wierczinski B, Yakushev A, Yeremin A (2006) Phys Rev Lett 97:242501-1-4

[5] Oganessian YT (2007) J Phys G 34:R165-R242

[6] Oganessian YT (2011) Radiochim Acta 99:429-439

[7] Oganessian YT, Abdullin FS, Alexander C, Binder J, Boll RA, Dmitriev SN, Ezold J, Felker K, Gostic JM, Grzywacz RK, Hamilton JH, Henderson RA, Itkis MG, Miernik K, Miller D, Moody KJ, Polyakov AN, Ramayya AV, Roberto JB, Ryabinin MA, Rykaczewski KP, Sagaidak RN, Shaughnessy DA, Shirokovsky IV, Shumeiko MV, Stoyer MA, Stoyer NJ, Subbotin VG, Sukhov AM, Tsyganov YS, Utyonkov VK, Voinov AA, Vostokin GK (2013) Phys Rev C87:054621-1-10

[8] Barber RC, Karol PJ, Nakahara H, Vardaci E, Vogt EW (2011) Pure Appl Chem 83(7):1485-1498

[9] Hofmann S, Ackermann D, Antalic S, Burkhard HG, Comas VF, Dressler R, Gan Z, Heinz S, Heredia JA, Heßberger FP, Khuyagbaatar J, Kindler B, Kojouharov I, Kuusiniemi P, Leino M, Lommel B, Mann R, Münzenberg G, Nishio K, Popeko AG, Saro S, Schött HJ, Streicher B, Sulignano B, Uusitalo J, Venhart M, Yeremin AV (2007) Eur Phys J A32:251-260

[10] Stavsetra L, Gregorich KE, Dvorak J, Ellison PA, Dragojević I, Garcia MA, Nitsche H (2009) Phys Rev Lett 103:132502-1-4

[11] Düllmann CE, Schädel M, Yakushev A, Türler A, Eberhardt K, Kratz JV, Ackermann D,

Andersson L-L, Block M, Brüchle W, Dvorak J, Essel HG, Ellison PA, Even J, Gates JM, Gorshkov A, Graeger R, Gregorich KE, Hartmann W, Herzberg R-D, Heßberger FP, Hild D, Hübner A, Jäger E, Khuyagbaatar J, Kindler B, Krier J, Kurz N, Lahiri S, Liebe D, Lommel B, Maiti M, Nitsche H, Omtvedt JP, Parr E, Rudolph D, Runke J, Schausten B, Schimpf E, Semchenkov A, Steiner J, Thörle-Pospiech P, Uusitalo J, Wegrzecki M, Wiehl N (2011) Phys Rev Lett 104:252701-1-5

[12] Gates JM, Düllmann CE, Schädel M, Yakushev A, Türler A, Eberhardt K, Kratz JV, Ackermann D, Andersson L-L, Block M, Brüchle W, Dvorak J, Essel HG, Ellison PA, Even J, Forsberg U, Gellanki J, Gorshkov A, Graeger R, Gregorich KE, Hartmann W, Herzberg R-D, Heßberger FP, Hild D, Hübner A, Jäger E, Khuyagbaatar J, Kindler B, Krier J, Kurz N, Lahiri S, Liebe D, Lommel B, Maiti M, Nitsche H, Omtvedt JP, Parr E, Rudolph D, Runke J, Schaffner H, Schausten B, Schimpf E, Semchenkov A, Steiner J, Thörle-Pospiech P, Uusitalo J, Wegrzecki M, Wiehl N (2011) Phys Rev C83:054618-1-17

[13] Hofmann S, Heinz S, Mann R, Maurer, Khuyagbaatar J, Ackermann D, Antalic S, Barth W, Block M, Burkhard HG, Comas VF, Dahl L, Eberhardt K, Gostic J, Henderson RA, Heredia JA, Heßberger FP, Kenneally JM, Kindler B, Kojouharov I, Kratz JV, Lang R, Leino M, Lommel B, Moody KJ, Münzenberg G, Nelson SL, Nishio K, Popeko AG, Runke J, Saro S, Shaughnessy DA, Stoyer MA, Thörle-Pospiech P, Tinschert K, Trautmann N, Uusitalo J, Wilk PA, Yeremin AV (2012) Eur Phys J A48:62-84

[14] Seaborg GT, Loveland WD (1990) The Elements Beyond Uranium. Wiley-Interscience, New York

[15] Herzberg R-D, Greenlees PT (2008) Prog Part Nucl Phys 61:674-720

[16] Bemis Jr CE, Silva RJ, Hensley DC, Keller Jr OL, Tarrant JR, Hunt LD, Dittner PF, Hahn RL, Goodman CD (1973) Phys Rev Lett 31:647-650

[17] Carlsson TA, Nestor Jr CW, Malik FB, Tucker TC (1969) Nucl Phys A135:57-64

[18] Moseley HGJ (1913) Phil Mag 26:1024-1034

[19] Rudolph D, Forsberg U, Golubev P, Sarmiento LG, Yakushev A, Andersson L-L, Di Nitto A, Düllmann CE, Gates JM, Gregorich KE, Gross CJ, Heßberger FP, Herzberg R-D, Khuyagbaatar J, Kratz JV, Rykaczewski K, Schädel M, Åberg S, Ackermann D, Block M, Brand H, Carlsson BG, Cox D, Derkx X, Eberhardt K, Even J, Fahlander C, Gerl J, Jäger E, Kindler B, Krier J, Kojouharov I, Kurz N, Lommel B, Mistry A, Mokry C, Nitsche H, Omtvedt JP,

Papadakis P, Ragnarsson I, Runke J, Schaffner H, Schausten B, Thörle-Pospiech P, Torres T, Traut T, Trautmann N, Türler A, Ward A, Ward DE, Wiehl N (2013) Phys Rev Lett 111:112502-1-5

[20] Oganessian YT, Utyonkoy VK, Lobanov YV, Abdullin FS, Polyakov AN, Shirokovsky IV, Tsyganov YS, Gulbekian GG, Bogomolov SL, Mezentsev AN, Iliev S, Subbotin VG, Sukhov AM, Voinov AA, Buklanov GV, Subotic K, Zagrebaev VI, Itkis MG, Patin JB, Moody KJ, Wild JF, Stoyer MA, Stoyer NJ, Shaughnessy DA, Kenneally JM, Lougheed RW (2004) Phys Rev C69:021601-1-5

[21] Oganessian YT, Abdullin FS, Dmitriev SN, Gostic JM, Hamilton JH, Henderson RA, Itkis MG, Moody KJ, Polyakov AN, Ramayya AV, Roberto JB, Rykaczewski KP, Sagaidak RN, Shaughnessy DA, Shirokovsky IV, Stoyer MA, Stoyer NJ, Subbotin VG, Sukhov AM, Tsyganov YS, Utyonkov VK, Voinov AA, Vostokin GK (2013) Phys Rev C87:014302-1-10

[22] Schädel M (2007) Eur Phys J D45:67-74

[23] Runke J, Düllmann CE, Eberhardt K, Ellison PA, Gregorich KE, Hofmann S, Jäger E, Kindler B, Kratz JV, Krier J, Lommel B, Mokry C, Nitsche H, Roberto JB, Rykaczewski KP, Schädel M, Thörle-Pospiech P, Trautmann N, Yakushev A (2014) J Radioanal Nucl Chem 299:1081-1084

[24] Andersson L-L, Rudolph D, Golubev P, Herzberg R-D, Hoischen R, Merchán E, Ackermann D, Düllmann CE, Eberhardt K, Even J, Gerl J, Heßberger FP, Jäger E, Khuyagbaatar J, Kojouharov I, Kratz JV, Krier J, Kurz N, Prokopowicz W, Schädel M, Schaffner H, Schausten B, Schimpf E, Semchenkov A, Türler A, Wollersheim H-J, Yakushev A, Thörle-Pospiech P, Hartmann W, Hübner A, Lommel B, Kindler B, Steiner J (2010) Nucl Instr Meth A622:164-170

[25] Rudolph D, Forsberg U, Golubev P, Sarmiento LG, Yakushev A, Andersson L-L, Di Nitto A, Düllmann CE, Gates JM, Gregorich KE, Gross CJ, Herzberg R-D, Heßberger FP, Khuyagbaatar J, Kratz JV, Rykaczewski K, Schädel M, Åberg S, Ackermann D, Block M, Brand H, Carlsson BG, Cox D, Derkx X, Eberhardt K, Even J, Fahlander C, Gerl J, Jäger E, Kindler B, Krier J, Kojouharov I, Kurz N, Lommel B, Mistry A, Mokry C, Nitsche H, Omtvedt JP, Papadakis P, Ragnarsson I, Runke J, Schaffner H, Schausten B, Thörle-Pospiech P, Torres T, Traut T, Trautmann N, Türler A, Ward A, Ward DE, Wiehl N (2014) Acta Phys Pol B45:263-272

[26] Forsberg U, Rudolph D, Golubev P, Sarmiento LG, Yakushev A, Andersson L-L, Di Nitto A, Düllmann CE, Gates JM, Gregorich KE, Gross CJ, Heßberger FP, Herzberg R-D, Khuyagbaatar J, Kratz JV, Rykaczewski K, Schädel M, Åberg S, Ackermann D, Block M, Brand H, Carlsson BG, Cox D, Derkx X, Eberhardt K, Even J, Fahlander C, Gerl J, Jäger E, Kindler B, Krier J, Kojouharov I, Kurz N, Lommel B, Mistry A, Mokry C, Nitsche H, Omtvedt JP, Papadakis P, Ragnarsson I, Runke J, Schaffner H, Schausten B, Thörle-Pospiech P, Torres T, Traut T, Trautmann N, Türler A, Ward A, Ward DE, Wiehl N (2014) Eur Phys J Web of Conferences 66:02036-1-4

[27] Forsberg U, Rudolph D, Andersson L-L, Di Nitto A, Düllmann CE, Gates JM, Golubev P, Gregorich KE, Gross CJ, Herzberg R-D, Heßberger FP, Khuyagbaatar J, Kratz JV, Rykaczewski K, Sarmiento LG, Schädel M, Yakushev A, Åberg S, Ackermann D, Block M, Brand H, Carlsson BG, Cox D, Derkx X, Eberhardt K, Even J, Fahlander C, Gerl J, Jäger E, Kindler B, Krier J, Kojouharov I, Kurz N, Lommel B, Mistry A, Mokry C, Nitsche H, Omtvedt JP, Papadakis P, Ragnarsson I, Runke J, Schaffner H, Schausten B, Thörle-Pospiech P, Torres T, Traut T, Trautmann N, Türler A, Ward A, Ward DE, Wiehl N () Phys Rev C:submitted

[28] Forsberg U, Golubev P, Sarmiento LG, Jeppsson J, Rudolph D, Andersson L-L, Ackermann D, Asai M, Block M, Düllmann CE, Dvorak J, Eberhardt K, Even J, Gates JM, Gregorich KE, Herzberg R-D, Heßberger FP, Jäger E, Khuyagbaatar J, Kojouharov I, Kratz JV, Krier J, Kurz N, Lahiri S, Lommel B, Maiti M, Merchán E, Omtvedt JP, Parr E, Runke J, Schaffner H, Schädel M, Yakushev A (2012) Acta Phys Pol B43:305-311

[29] Khuyagbaatar J, Ackermann D, Andersson L-L, Ballof J, Brüchle W, Düllmann CE, Dvorak J, Eberhardt K, Even J, Gorshkov A, Graeger R, Heßberger FP, Hild D, Hoischen R, Jäger E, Kindler B, Kratz JV, Lahiri S, Lommel B, Maiti M, Merchán E, Rudolph D, Schädel M, Schaffner H, Schausten B, Schimpf E, Semchenkov A, Serov A, Türler A, Yakushev A (2012) Nucl Instr Meth A689:40-46

[30] Kibédi T, Trzhaskovskaya MB, Gupta M, Stuchbery AE (2012) At Data Nucl Data Tables 98:313-355

[31] Heßberger FP, Hofmann S, Münzenberg G, Schmidt K-H, Armbruster P, Hingmann R (1989) Nucl Instr Meth A274:522-527

[32] Sarmiento LG, Andersson L-L, Rudolph D (2012) Nucl Instr Meth. A667:26-31

[33] Sarmiento LG, Rudolph D, Forsberg U, Golubev P, Andersson L-L () Proc Science:submitted.

[34] Möller P, Nix JR, Myers WD, Swiatecki WJ (1995) At Data Nucl Data Tables 59:185-381

[35] Goriely S, Tondeur F, Pearson JM (2001) At Data Nucl Data Tables 77:311-381

[36] Geng LS, Toki H, Meng J (2003) Phys Rev C68:061303-1-5

[37] Muntian I, Hofmann S, Patyk Z, Sobiczewski A (2003) Acta Phys Pol B34:2073-2082; Muntian I, Patyk Z, Sobiczewski A (2003) Phys At Nucl 66:1015-1019

[38] Tolokonnikov SV, Lutostansky YS, Saperstein EE (2013) Phys At Nucl 76:708-715

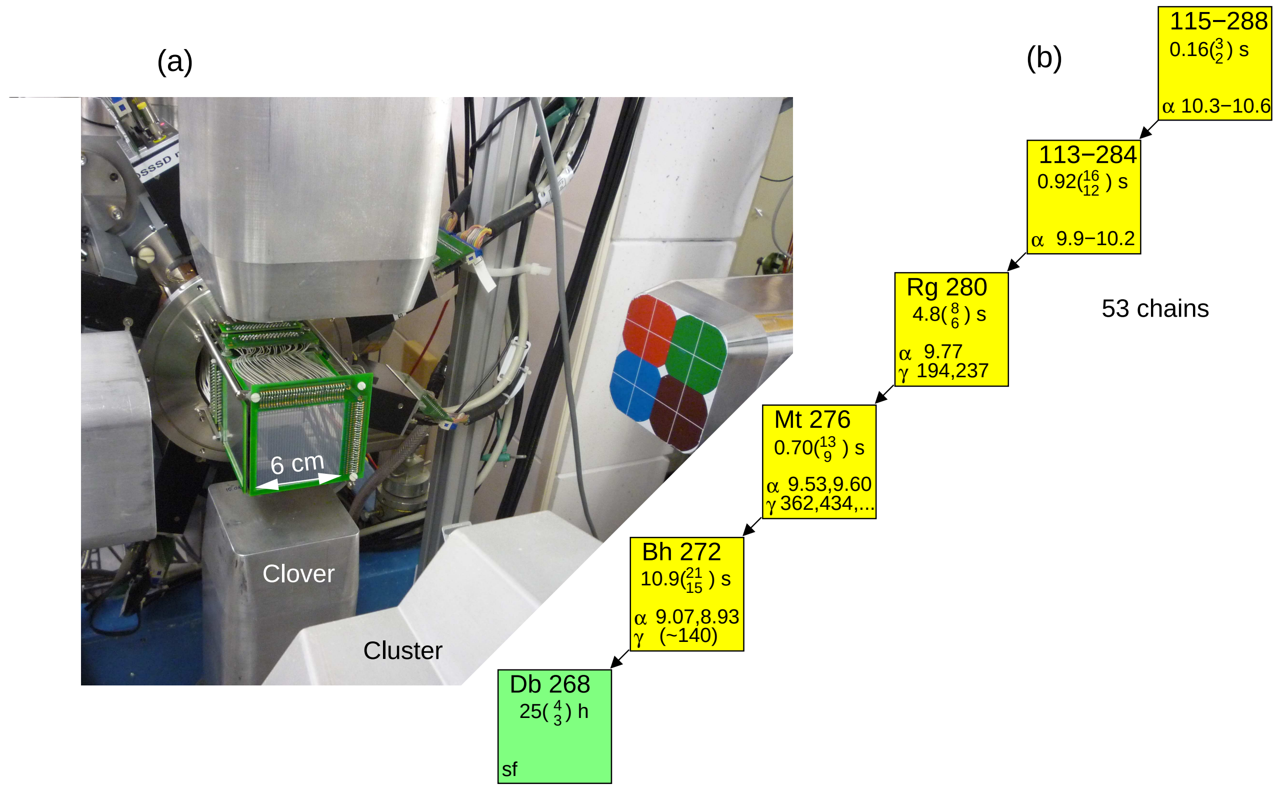

FIG. 1: Colour online: (a) Photograph of the TASISpec α-photon coincidence set-up [24] in the focal plane of the TASCA gas-filled separator at GSI [22]. See text for details. (b) Proposed decay chain of $^{288}115$ based on the combined data of Refs. [19–21].

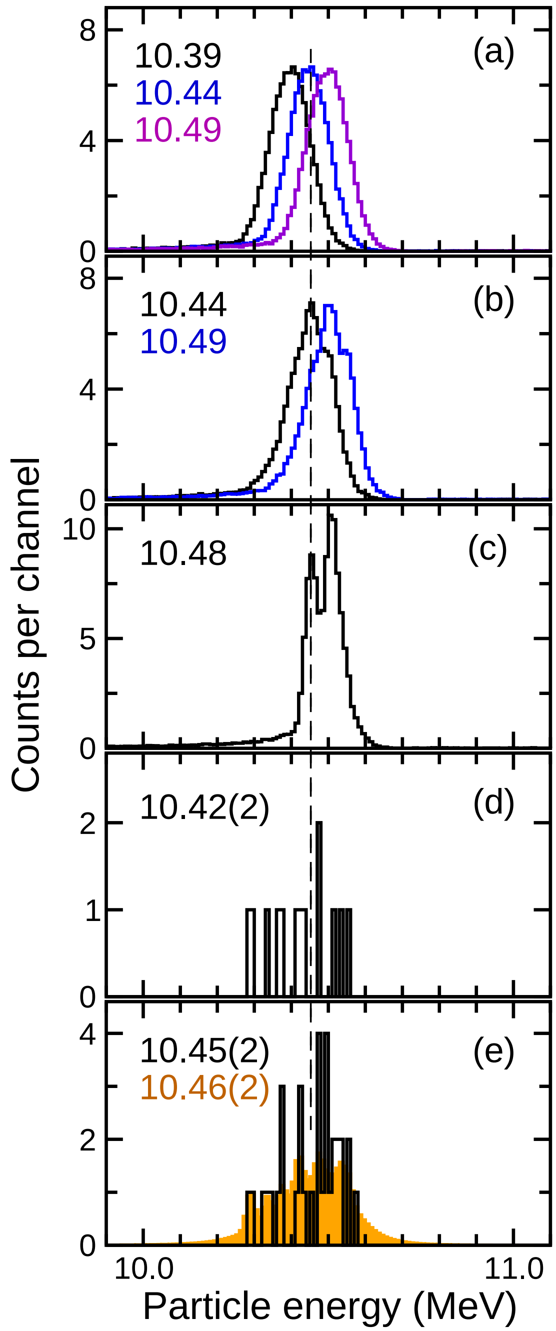

FIG. 2: Colour online: (a)-(c) Particle energy spectra resulting from various TASISpec Monte-Carlo simulations [32] employing different Q_α values and/or decay schemes of the decay of $^{288}115$ (cf. Fig. 3). (d) Experimental particle energy spectrum of the α decay of $^{288}115$ [19]. (e) Experimental particle energy spectrum (black) and distribution (orange) of the α decay of $^{288}115$ using combined data of Refs. [19–21]. The numbers in each panel reflect the mean value of the spectra in the interval [10.2,10.8] MeV. A dashed line at 10.45 MeV is indicated to guide the eye. The binning is 10 keV per channel. See text for more details.

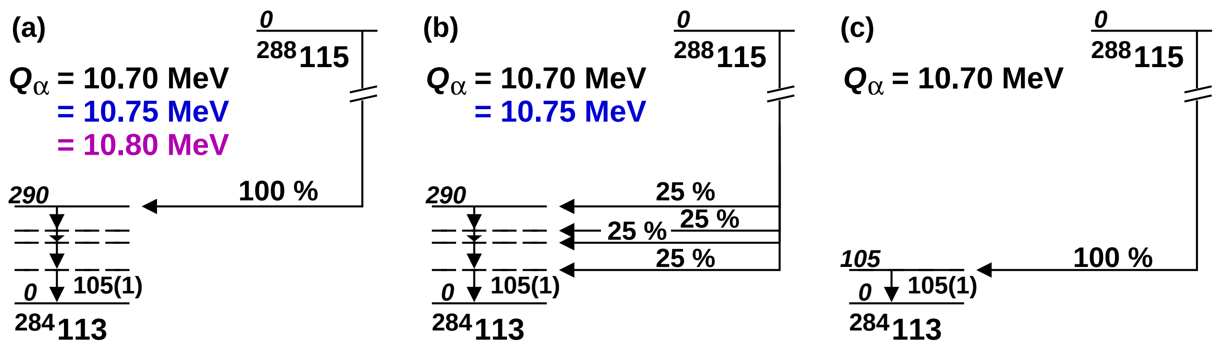

FIG. 3: Colour online: Various decay schemes of $^{288}115$ used as input for TASISpec Monte Carlo simulations [32]. Here, panels (a) through (c) refer to panels (a) to (c) in Fig. 2. Denoted Q_α values are ground state-to-ground state measures.

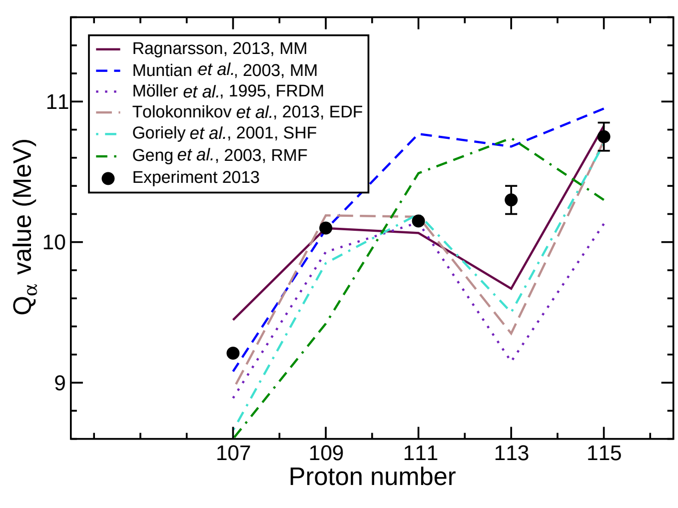

FIG. 4: Colour online: Comparison of experimental Q_α values of the $^{288}115$ decay chain (black dots) with predictions of various nuclear structure models.